

Simple Coumarin-Based Fluorescent Probe for Recognition of Pd(II) and Its Live Cell Imaging

Xiangyang Zhang,* Yaodan Xu, Youming Shen, and Feifei Wang*

Cite This: *ACS Omega* 2023, 8, 35121–35126

Read Online

ACCESS |



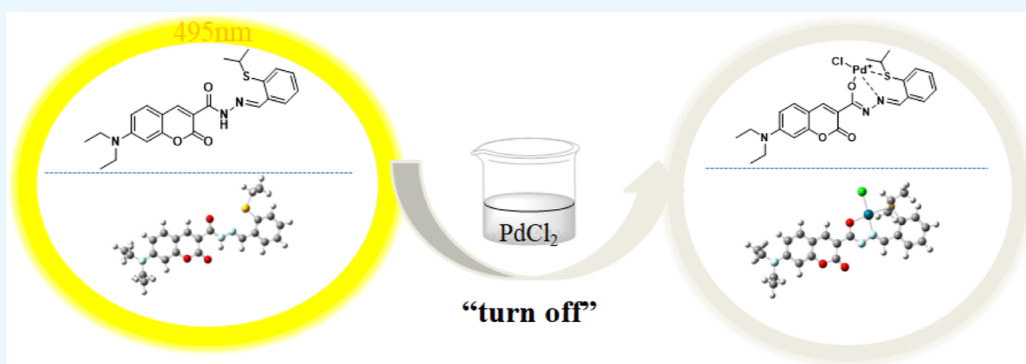
Metrics & More



Article Recommendations



Supporting Information



ABSTRACT: A simple coumarin hydrazine Schiff base bearing a thioether recognition fragment (compound CBBS) has been rationally designed and easily prepared. CBBS exhibited an excellent selectivity for Pd(II) and a low detection limit of 65 nM (S/N = 3). The fluorescence emission intensities of CBBS at 495 nm were linear to Pd(II) concentrations in a wide range from 0 to 80 μ M. Moreover, CBBS has been well used in fluorescence imaging of Pd(II) in living A549 cells. CBBS as a simple coordination-based fluorescent probe will inspire the researchers to develop a polymer for selective detection and adsorption of Pd(II).

1. INTRODUCTION

Palladium(II), one of the biological toxicity metal ions, can cause eye irritations, skin cancer, and several cellular processes and biological activity disorders.¹ However, they have wide industrial applications, such as pharmaceuticals,² fuel cells,³ manufacturing electrical products,⁴ and so on. In this case, people are easily exposed to palladium(II) ions and susceptible to poisoning.⁵ Moreover, owing to the maximum intake of palladium(II) ions being less than 15 μ g/day/person, various research studies have emphasized that we should reduce the risk of contact palladium(II) ions.^{6,7} Consequently, developing easily operational and efficient detection methods for palladium(II) ions in environmental and biological samples is rather necessary.

Recently, fluorometry has been one of the focuses in the detection of toxic matters.⁸ Fluorescence-based methods for detecting palladium(II) ions are competitive with conventional techniques because we do not suffer from expensive instrumentation, complicated operations, and highly skilled operation skills.^{9–11} Up to now, researchers have developed various fluorescent probes for recognition of palladium(II) ions.^{12,13} However, most of them were reactive fluorescence probes.¹⁴ As another type of fluorescence probe, coordination-based fluorescent probes are of great interest because they are privileged building blocks for preparing fluorescent polymers capable of selective adsorption of metal ions.¹⁵ Additionally,

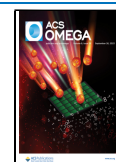
coordination-based fluorescent probes containing a Schiff base fragment possess remarkable advantages, such as simple synthesis route, lower cost, and available raw materials.¹⁶ Based on the above research background, we plan to develop a simple Schiff base for sensing palladium(II) ions.

Sulfide fragments can easily form a coordination bond between the sulfur atom and transition-metal ion, which is an attractive feature. For example, Faiges *et al.* disclosed that the thioether group of Ir/P,S-catalyst played a key role in directing the olefin coordination.¹⁷ Diéguez *et al.* have highlighted the catalytic performance of phosphorus–thioether ligand libraries.¹⁸ Mirica *et al.* reported one kind of heteroleptic mononuclear Pd(I) complex with high activity for C sp³–H bond activation.¹⁹ In that case, sulfur-containing recognition fragments would be beneficial for designing simple coordination-based fluorescent probes. However, the recognition abilities of simple fluorescent probes based on coumarin

Received: June 28, 2023

Accepted: August 31, 2023

Published: September 12, 2023



hydrazine Schiff bases containing thioether fragments for harmful heavy ions have not been systemically studied.

The construction of coordination-based coumarin fluorescent probes for detecting metal ions is a highly topical research field because of their ease of modification, relatively high-fluorescence quantum yield, and molar absorption coefficient.^{20,21} However, there are few examples of coordination-based coumarin fluorescent probes for detecting palladium(II) ions.^{22,23} Under this background, we begin to evaluate the sensing performance of an easily prepared coumarin Schiff base containing a thioether recognition fragment (compound CBBS) for palladium(II) ions. Furthermore, revealing the spectral properties of a coumarin-based fluorescence molecule with a thioether fragment could guide the design of the other coordination-based fluorescence probes for sensing metal ions.

2. RESULTS AND DISCUSSION

2.1. Spectroscopic Properties of CBBS. As illustrated in Figure 1, the UV–vis absorption spectrum of CBBS before and

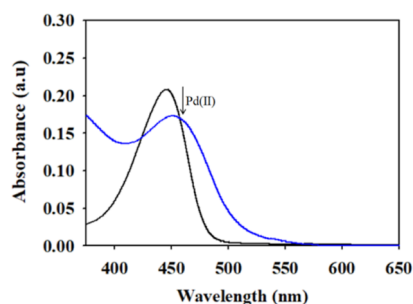


Figure 1. UV absorption changes of CBBS (10 μM) upon the addition of Pd(II) (80 μM) in phosphate-buffered saline (PBS)/dimethyl sulfoxide (DMSO) buffer solution (80/20, v/v, pH 7.4, 25 mM).

after the addition of 80 μM Pd(II) was investigated, respectively. Upon the addition of 80 μM Pd(II) (blue line), there was a marked decline in the UV absorption intensity ($\lambda_{\text{max}} = 450$ nm) of CBBS. Meanwhile, a redshift maximum absorption could be observed upon the addition of 80 μM Pd(II) to CBBS.

Next, we turned our attention to understand the fluorescence properties of CBBS with different concentrations of Pd(II) (0–80 μM) (Figure 2a). Obviously, the fluorescence emission intensity of CBBS at 495 nm gradually decreased

with the increase of Pd(II) concentration. The fluorescence emission intensity of CBBS was at the lowest level, when 80 μM Pd(II) ions were added into the aqueous media containing CBBS (Figure 2a). The fluorescence emission intensity at 495 nm was proportional to the Pd(II) concentrations linearly in 0–80 μM (Figure 2b). The regression equations are $F_1 = 7763.9 - 155.33 \times [\text{Pd}^{2+}]$ (0–40 μM , $R^2 = 0.990$) and $F_2 = 3118.4 - 30.66 \times [\text{Pd}^{2+}]$ (40–80 μM , $R^2 = 0.995$). Moreover, the detection limit of CBBS was calculated to be 6.5×10^{-8} M ($S/N = 3$). These results suggested that CBBS as a fluorescent probe for detecting Pd(II) was acceptable.

2.2. Fluorescence Properties of CBBS toward Metal Ions. Furthermore, the fluorescent responses of CBBS toward different metal ions were investigated in PBS/DMSO buffer solution (80/20, v/v, pH 7.4, 25 mM). After adding 80 μM of the other ions (Mg^{2+} , Co^{2+} , Cu^{2+} , Mn^{2+} , Zn^{2+} , Ni^{2+} , Pb^{2+} , Hg^{2+} , La^{3+} , Al^{3+} , Rh^{3+} , Cr^{3+} , Fe^{3+} , and Cd^{2+}) to the CBBS solution (10 μM), we did not observe the apparent changes of fluorescence intensity ratio (I/I_0) at 495 nm (Figure 3). This phenomenon indicated that CBBS had a high selectivity for detecting Pd(II).

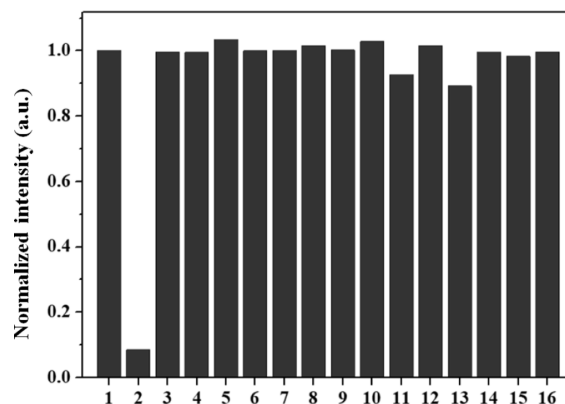


Figure 3. Fluorescence response of CBBS (10 μM) against various metal ions (80 μM); 1 = blank, 2 = Pd^{2+} , 3 = Mg^{2+} , 4 = Co^{2+} , 5 = Cu^{2+} , 6 = Mn^{2+} , 7 = Zn^{2+} , 8 = Ni^{2+} , 9 = Pb^{2+} , 10 = Hg^{2+} , 11 = La^{3+} , 12 = Al^{3+} , 13 = Rh^{3+} , 14 = Cr^{3+} , 15 = Fe^{3+} , and 16 = Cd^{2+} ; $\lambda_{\text{em}} = 495$ nm.

2.3. Effect of pH and Response Time of CBBS. As shown in Figure 4, in a pH range of 4.0–10.0, the fluorescence intensity of CBBS was high (solid line). Obviously, once 80 μM Pd(II) was added to the PBS/DMSO buffer solution containing CBBS, the fluorescence intensity of CBBS solution

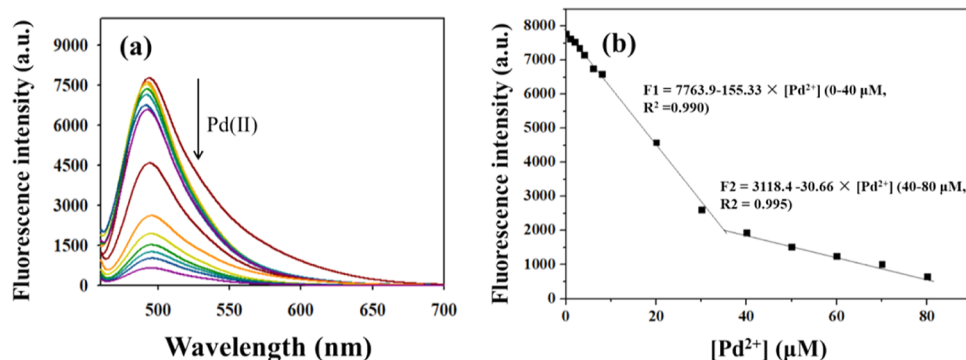


Figure 2. (a) Fluorescence spectra of CBBS (10 μM) upon the addition of Pd(II) (0–80 μM) in PBS/DMSO buffer solution (80/20, v/v, pH 7.4, 25 mM). (b) Fluorescence emission intensity of CBBS at 495 nm vs the concentration of Pd(II) ($\lambda_{\text{ex}} = 450$ nm).

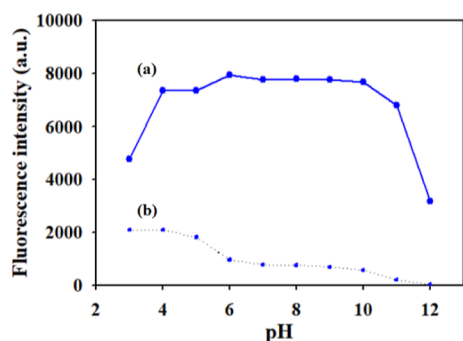


Figure 4. Effect of pH values on the fluorescence intensity of CBBS (10 μM) in the absence (solid line) and presence of 80 μM Pd(II) (dashed line).

had a largest decrease in the range of pH 4–10 (dashed line). This finding showed that CBBS as a fluorescence probe for Pd(II) could keep a stable detection performance within a wide range of pH values.

For preliminary understanding the kinetic property of CBBS after adding Pd(II), the response time was evaluated (Figure 5). We first confirmed that the fluorescence intensity of CBBS

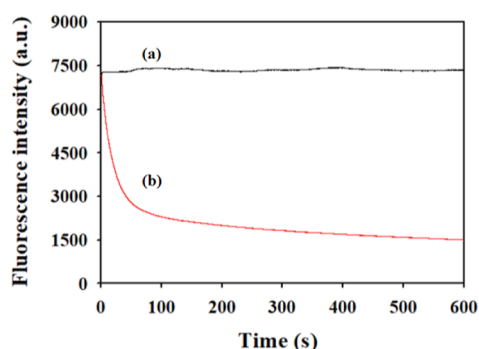


Figure 5. Time profile of CBBS (10 μM) in the absence (line a, black) and presence of 80 μM Pd(II) (line b, red) in PBS/DMSO buffer solution (80/20, v/v, pH 7.4, 25 mM).

itself was stable (line a). Also then, it was observed that when 80 μM Pd(II) was added to the detection system, the fluorescence intensity of CBBS at 495 nm decreased rapidly (line b) and tended to be stable in a short time (600 s). This findings suggested that CBBS could detect Pd(II) quickly.

2.4. Binding Mechanism and DFT Calculation. As shown in Figure 6, the electrospray ionization-mass spectrometry (ESI-MS) spectra of complex CBBS–Pd(II) showed a peak at

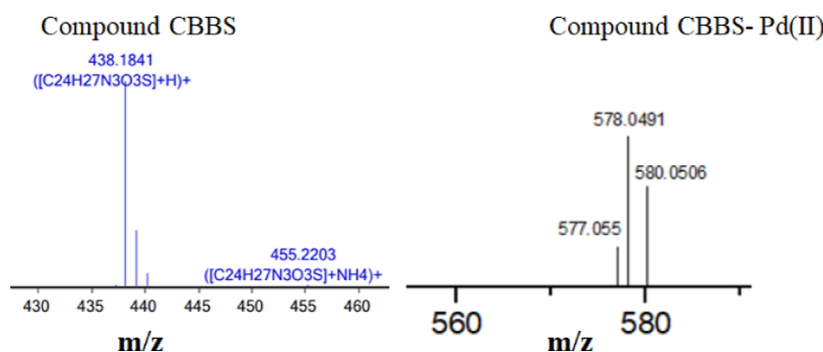


Figure 6. ESI-MS spectra of CBBS and complex CBBS–Pd(II).

m/z 578.0491, which matched the calculated value of m/z 578.0486 ($\text{C}_{24}\text{H}_{27}\text{ClN}_3\text{O}_3\text{SPd}^+$). For gaining the other evidence about the binding model, Job's plot of CBBS–Pd(II) was also performed (Figure S3). An intermediate fluorescence intensity at 495 nm was observed when the molecular fraction of Pd(II) was 0.5, indicating the 1:1 binding of CBBS with Pd(II).

Beyond that, we have used the long-range separated hybrid functional CAM-B3LYP with def2-SVP basis to optimize the geometry and calculate the excited state property of CBBS and complex CBBS–Pd(II), respectively (Figure 7). The calcu-

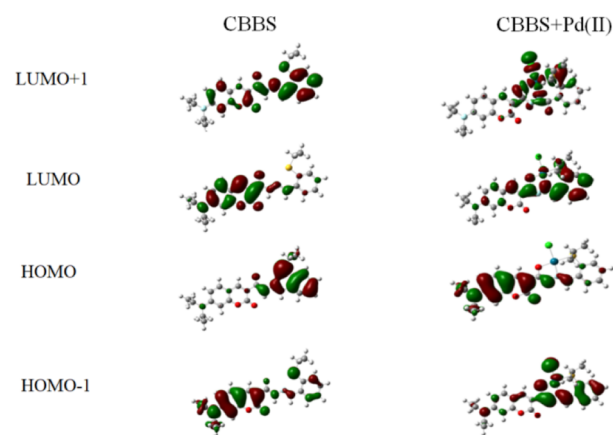


Figure 7. Frontier molecular orbital profiles of CBBS and complex CBBS–Pd(II) obtained from the density functional theory (DFT) (CAM-d3LYP/def2SVP) calculations.

lated oscillator strength (f) of CBBS was 1.27, which was much larger than the 0.01 of CBBS–Pd(II). This data indicated that Pd(II) could quench fluorescence of CBBS from the perspective of theoretical calculation. According to the above data, a possible binding model of CBBS with Pd(II) was proposed (Scheme 1).

2.5. Imaging in Cells. For checking the potential bio-applications of CBBS, imaging of Pd(II) ions in A549 cells was preliminarily studied (for the experiment details, see the Supporting Information). In the yellow channel (470–600 nm), a fluorescence signal was observed when living A549 cells were incubated with 10 μM CBBS for 30 min (Figure 8a). When 80 μM Pd(II) ions were added to A549 cells pretreated with N-ethylmaleimide (NEM) and preincubated with CBBS successively, a weak fluorescence signal was observed an hour later (Figure 8c). In addition, the toxicity of CBBS on A549 cells was investigated using the 3-[4,5-dimethylthiazol-2-yl]-2,5

Scheme 1. Proposed Binding Mechanism of CBBS toward Pd(II)

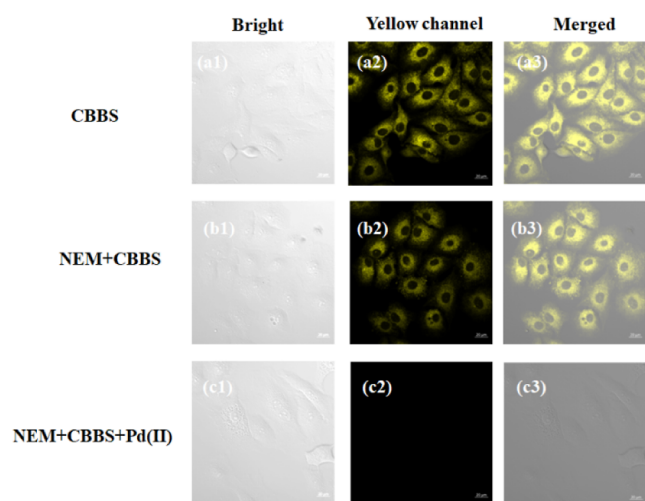
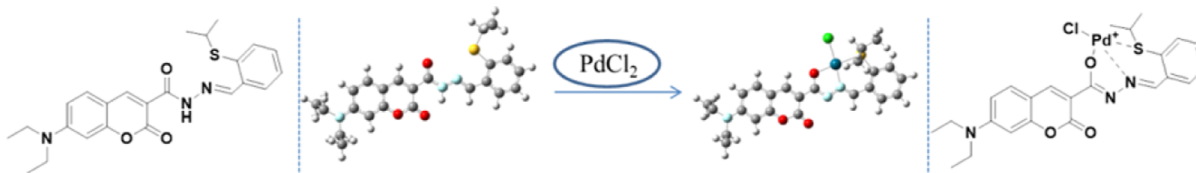


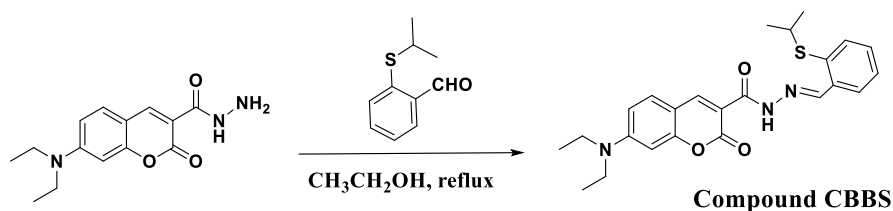
Figure 8. Fluorescence images of A549 cells incubated with CBBS for 30 min. (a1–a3) Fluorescence images of A549 cells pretreated with NEM (1.0 mmol/L) for 30 min and then incubated with CBBS for 30 min (b1–b3) and those first incubated with NEM and CBBS, respectively, for 30 min, and then incubated with Pd(II) for 60 min (c1–c3).

diphenyl tetrazolium bromide method (Figure S5). After 12 or 24 h of incubation with 10 μM CBBS, the survival rate of A549 cells is still very high. These results indicated that CBBS as a coumarin-based fluorescent probe for imaging of Pd(II) ions in A549 cells was practicable.

3. CONCLUSIONS

A simple coumarin Schiff base-based fluorescent probe named CBBS was successfully developed. The linear fashion of the fluorescence intensity decline of CBBS with the concentration of Pd(II) could be applied in the quantification of Pd(II) in aqueous solution. A possible binding model of CBBS with Pd(II) was studied *via* high-resolution (HR)-MS, Job's plots, and DFT calculation. Moreover, CBBS could be applied in identifying Pd(II) in living A549 cells. This study has enriched the luminous family of coumarin-based Schiff bases bearing a thioether fragment.

Scheme 2. Syntheses of Compound CBBS



4. EXPERIMENTAL SECTION

4.1. Reagents and Apparatus. 2-Fluorobenzaldehyde, isopropyl mercaptan, 4-(diethylamino)salicylaldehyde, and ethanol were provided by Energy-Chemical Reagent Co., Ltd. A 5.0 mM stock solution of PdCl₂ and RhCl₃·3H₂O was both prepared in the cosolvent solution (brine/methanol, 1:3, v/v). The solutions of various metal ions were obtained from MgCl₂·6H₂O, CoCl₂·6H₂O, CuCl₂·2H₂O, MnSO₄, Zn(NO₃)₂·7H₂O, NiSO₄·6H₂O, PbCl₂, HgCl₂, LaCl₃·7H₂O, Al₂(SO₄)₃, CrCl₃·6H₂O, FeCl₃·6H₂O, and CdCl₂·2.5H₂O using ultrapure water. The melting point of CBBS was tested in an X-4B instrument (Yidian Physical Optical Instrument Co., Ltd, China). NMR measurements were performed on a Bruker AVB-400 MHz spectrometer (Switzerland). The HR-MS analyses were carried out on a Bruker solanX 70 Fourier transform (FT)-MS. UV–vis absorption spectra were investigated by a Shimadzu UV-2450 (Japan). Fluorescence properties of CBBS were studied by a Hitachi F-7000 (Japan) with setting both excitation slit and emission slit to 5 nm. Frontier molecular orbital profiles of CBBS and CBBS–Pd(II) complexes based on the DFT (CAM-d3LYP/def2SVP) calculations were conducted in the framework of the Gaussian 09 program.

4.2. Preparation of Compound CBBS. The synthesis of compound CBBS is summarized in Scheme 2. 2-(Isopropylthio)benzaldehyde and 7-(diethylamino)-2-oxo-2H-chromene-3-carbohydrazide (coumarin hydrazine) were easily synthesized according to previously reported methods, respectively.^{24,25} Compound CBBS was synthesized by a condensation reaction of coumarin hydrazine (1.4 g, 5.0 mmol) with 2-(isopropylthio)benzaldehyde (1.0 g, 5.5 mmol) in 20.0 mL of absolute ethanol. Under nitrogen, the reaction solution refluxed in an oil bath for 12 h and cooled to room temperature. Finally, a yellow solid compound CBBS was obtained through column chromatography (dichloromethane as the eluent) (1.9 g, 86% yield). m.p. 187 °C; ¹H NMR (400 MHz, CDCl₃): δ (ppm) 11.92 (s, 1H), 8.78 (s, 1H), 8.23 (s, 1H), 7.51–7.49 (d, *J* = 8 Hz, 2H), 7.34–7.33 (m, 2H), 6.74–6.72 (m, 1H), 6.59 (s, 1H), 3.51–3.46 (m, 4H), 3.30–3.24 (m, 1H), 1.35–1.26 (q, 6H), 1.25–1.20 (q, 6H); ¹³C NMR (100 MHz, CDCl₃): δ (ppm) 162.8, 159.9, 157.8, 152.9, 149.2, 147.2, 136.0, 135.4, 131.4, 130.3, 127.9, 127.6, 127.5, 110.3,

109.1, 108.7, 96.7, 45.2, 40.1, 23.1, 12.4; HR-MS (ESI⁺, *m/z*): [M + H]⁺ calcd for C₂₄H₂₈N₃O₃S, 438.1846; found, 438.1841.

■ ASSOCIATED CONTENT

SI Supporting Information

The Supporting Information is available free of charge at <https://pubs.acs.org/doi/10.1021/acsomega.3c04626>.

¹H NMR, ¹³C NMR, and HR-MS spectra for CBBS; Job's plot diagram of CBBS for Pd²⁺; experimental process of A549 cell culture; survival of A549 cells in 10 μM CBBS in 12 or 24 h; and dominant conformation of CBBS and CBBS–Pd(II) (PDF)

■ AUTHOR INFORMATION

Corresponding Authors

Xiangyang Zhang – College of Chemistry and Material Engineering, Hunan University of Arts and Science, Changde 415000, P. R. China; Changde Engineering Technology Research Center of Biomedical Polymer Materials, Changde 415000, P. R. China; orcid.org/0000-0002-8465-425X; Email: zhangxiangy06@163.com

Feifei Wang – College of Chemistry and Material Engineering, Hunan University of Arts and Science, Changde 415000, P. R. China; Changde Engineering Technology Research Center of Biomedical Polymer Materials, Changde 415000, P. R. China; Email: Wangfeifei3597@163.com

Authors

Yaodan Xu – College of Chemistry and Material Engineering, Hunan University of Arts and Science, Changde 415000, P. R. China; Changde Engineering Technology Research Center of Biomedical Polymer Materials, Changde 415000, P. R. China

Youting Shen – College of Chemistry and Material Engineering, Hunan University of Arts and Science, Changde 415000, P. R. China; Changde Engineering Technology Research Center of Biomedical Polymer Materials, Changde 415000, P. R. China; orcid.org/0000-0001-5806-9551

Complete contact information is available at: <https://pubs.acs.org/10.1021/acsomega.3c04626>

Notes

The authors declare no competing financial interest.

■ ACKNOWLEDGMENTS

This research received financial support from the Hunan Provincial Natural Science Foundation of China (HPNCF, 2020JJ4445).

■ REFERENCES

- (1) Wiseman, C. L.; Zereini, F. Airborne particulate matter, platinum group elements and human health: a review of recent evidence. *Sci. Total Environ.* **2009**, *407*, 2493–2500.
- (2) Zhang, Y. D.; White, J. A. H.; Chong, E.; Radomkit, S.; Xu, Y. B.; Liu, J.; Lorenz, J. C. Development of Pd-catalyzed asymmetric allylic alkylation with low catalyst loading for large-scale production of ethyl (*R*)-1-allyl-2-oxocyclohexane-1-carboxylate. *Org. Process Res. Dev.* **2023**, *27*, 1406–1410.
- (3) Sarkar, S.; Peter, S. C. An overview on Pd-based electrocatalysts for the hydrogen evolution reaction. *Inorg. Chem. Front.* **2018**, *5*, 2060–2080.
- (4) Che, C. L.; Chen, X. Z.; Wang, H. M.; Li, J.-Q.; Xiao, Y. M.; Fu, B.; Qin, Z. H. A novel 6-quinoxalinamine-based fluorescent probe for

real-time detection of palladium(II) ions in pure water and bioimaging. *New J. Chem.* **2018**, *42*, 12773–12778.

(5) *International Programme on Chemical Safety, Palladium*; Environmental Health Criteria Series 226; World Health Organization: Geneva, 2002.

(6) Xiang, J. J.; Liu, C. J.; Zhou, L. H.; Yang, X.; Li, Y.; Jiang, Y. C.; Mahmood, T.; Zhang, P. F.; Gong, P.; Cai, L. T. Ratiometric photoacoustic chemical sensor for Pd²⁺ ion. *Anal. Chem.* **2020**, *92*, 4721–4725.

(7) Li, H. L.; Fan, J. L.; Peng, X. J. Colourimetric and fluorescent probes for the optical detection of palladium ions. *Chem. Soc. Rev.* **2013**, *42*, 7943–7962.

(8) Han, T.; Zhu, S. M.; Wang, S. C.; Wang, B. J.; Zhang, X. J.; Wang, G. F. Fluorometric methods for determination of H₂O₂, glucose and cholesterol by using MnO₂ nanosheets modified with 5-carboxyfluorescein. *Microchim. Acta* **2019**, *186*, 269.

(9) Adak, A. K.; Dutta, B.; Manna, S. K.; Sinha, C. Rhodamine-appended benzophenone probe for trace quantity detection of Pd²⁺ in living cells. *ACS Omega* **2019**, *4*, 18987–18995.

(10) Xu, F.; Zhang, D. K.; Lu, Q. Y.; Zhang, R.; Xia, J. B. Rational design of fluorescent chemosensor for Pd²⁺ based on the formation of cyclopalladated complex. *Talanta* **2023**, *253*, 123967.

(11) Jin, M.; Wei, L. H.; Yang, Y. T.; Run, M. T.; Yin, C. X. A new turn-on fluorescent probe for the detection of palladium(0) and its application in living cells and zebrafish. *New J. Chem.* **2019**, *43*, 548–551.

(12) Shally, Kumar, V.; Althagafi, I.; Kumar, A.; Singhal, D.; Kumar, A.; Gupta, R.; Pratap, R. Design and synthesis of new functionalized 8-(thiophen-2-yl)-1,2,3,4-tetrahydroquinolines as turn-off chemosensors for selective recognition of Pd²⁺ ions. *New J. Chem.* **2020**, *44*, 15559–15566.

(13) Wang, L.; Zheng, X.-Y.; Zhang, X.; Zhu, Z.-J. A quinoline-based fluorescent chemosensor for palladium ion (Pd²⁺)-selective detection in aqueous solution. *Spectrochim. Acta, Part A* **2021**, *249*, 119283.

(14) Huo, F. J.; Zhang, Y. Q.; Kang, J.; Chao, J. B.; Zhang, Y. B.; Yin, C. X. A novel alkyne compound as a Pd(II) fluorescent probe in aqueous medium and its bioimaging. *Sens. Actuators, B* **2017**, *243*, 429–434.

(15) Oshchepkov, A. S.; Oshchepkov, M. S.; Oshchepkova, M. V.; Al-Hamry, A.; Kanoun, O.; Kataev, E. A. Naphthalimide-based fluorescent polymers for molecular detection. *Adv. Opt. Mater.* **2021**, *9*, 2001913.

(16) Goshisht, M. K.; Patra, G. K.; Tripathi, N. Fluorescent Schiff base sensors as a versatile tool for metal ion detection: strategies, mechanistic insights, and applications. *Mater. Adv.* **2022**, *3*, 2612–2669.

(17) Faiges, J.; Borràs, C.; Pastor, I. M.; Pàmies, O.; Besora, M.; Diéguez, M. Density functional theory-inspired design of Ir/P,S-catalysts for asymmetric hydrogenation of olefins. *Organometallics* **2021**, *40*, 3424–3435.

(18) Margalef, J.; Pàmies, O.; Pericàs, M. A.; Diéguez, M. Evolution of phosphorus-thioether ligands for asymmetric catalysis. *Chem. Commun.* **2020**, *56*, 10795–10808.

(19) Tran, G. N.; Bouley, B. S.; Mirica, L. M. Isolation and characterization of heteroleptic mononuclear palladium(I) complexes. *J. Am. Chem. Soc.* **2022**, *144*, 20008–20015.

(20) Chen, H.; Zhou, Z.; Li, Z. Y.; He, X. J.; Shen, J. L. Highly sensitive fluorescent sensor based on coumarin organic dye for pyrophosphate ion turn-on biosensing in synovial fluid. *Spectrochim. Acta, Part A* **2021**, *257*, 119792.

(21) Xie, Y. T.; Cheng, W. J.; Jin, B.; Liang, C. G.; Ding, Y. B.; Zhang, W. H. Solvent directed selective and sensitive fluorescence detection of target ions using a coumarin-pyridine probe. *Analyst* **2018**, *143*, 5583–5588.

(22) Chen, X. Z.; Wang, H. M.; Ma, X. D.; Wang, M.; Zhang, Y. Y.; Gao, G.; Liu, J. J.; Hou, S. C. Colorimetric and fluorescent probe for real-time detection of palladium (II) ion in aqueous medium and live cell imaging. *Dyes Pigm.* **2018**, *148*, 286–291.

(23) Ren, A. M.; Zhang, Y.; Yu, W. W.; Zhao, K.; Hu, Z. R.; Zhang, Z. Q.; Feng, G. D.; Song, Z. G. Developed a high-performance sensor based on coumarin derivative for rapid and sensitive detection of palladium ion in organic wastewater. *J. Ind. Eng. Chem.* **2021**, *99*, 292–298.

(24) Kost, T.; Sigalov, M.; Goldberg, I.; Ben-Asuly, A.; Lemcoff, N. G. Latent sulfur chelated ruthenium catalysts: Steric acceleration effects on olefin metathesis. *J. Organomet. Chem.* **2008**, *693*, 2200–2203.

(25) Long, L.; Wu, Y. J.; Wang, L.; Gong, A. H.; Hu, F. L.; Zhang, C. A fluorescent probe for hypochlorite based on the modulation of the unique rotation of the N-N single bond in acetohydrazide. *Chem. Commun.* **2015**, *51*, 10435–10438.